Electronic Supplementary information

Site-selective bromination of anthracene–maleimide Diels-Alder crystals for tunable afterglow and white light emission

Guangxin Yang, Tianwen Zhu, Xiang Chen, Junhao Duan, Zhipeng Zhao, and Wang Zhang Yuan*

School of Chemistry and Chemical Engineering, Frontiers Science Center for Transformative Molecules, Shanghai Key Lab of Electrical Insulation and Thermal Aging, Shanghai Jiao Tong University, No. 800 Dongchuan Rd., Minhang District, Shanghai 200240, China.
E-mail: wzhyuan@sjtu.edu.cn

Experimental Section

Materials. 9-Bromoanthracene (BAN, >98.0%) and 3-bromomaleimide (BMI, 98.0%) were purchased from Adamas Reagent Co., Ltd. Maleimide (MI, 98.0%), 3,4-dibromomaleimide (DBMI, >98.0%), and 2-methyltetrahydrofuran (MTHF, ≥99.0%) were obtained from Shanghai Aladdin Biochemical Technology Co., Ltd. 9,10-Dibromoanthracene (DBAN, 98.5%) was supplied by Anhui Zesheng Technology Co., Ltd., and anthracene (AN, 99.0%) was purchased from Shanghai Meryer Chemical Technology Co., Ltd. Dichloromethane (DCM) and toluene were obtained from Shanghai Titan Scientific Co., Ltd. Chloroform ($CHCl_3$) and acetone were purchased from Sinopharm Chemical Reagent Co., Ltd. Unless otherwise specified, the above reagents and solvents are used directly without special treatment.

Instrumentation. ^{1}H and ^{13}C NMR spectra were recorded on a DRX-500 spectrometer (Bruker, Germany) at resonance frequencies of 500 and 126 MHz, respectively, using DMSO-d_6 as the solvent. Photophysical properties, including prompt and delayed emission spectra as well as luminescence lifetimes, were measured on an FLS1000 steady-state/transient fluorescence spectrometer (Edinburgh Instruments, UK) equipped with a PMT-900 detector at 298 K or 77 K. Absolute photoluminescence quantum yields (Φ) were determined using an integrating sphere (SPEKTRON-R98, φ=80 mm) on a QM/TM/IM steady-state and transient fluorescence measurement system (PTI, USA). UV–vis absorption spectra were recorded on a Lambda 750s spectrophotometer (PerkinElmer, USA). Photographs were taken using an α7s II digital camera (Sony, Japan). Single-crystal X-ray diffraction (SCXRD) data were collected on a D8 Venture-CMOS diffractometer (Bruker, Germany). The structures were solved and refined using the APEX3 software package and the SHELXTL program suite. High-resolution mass spectra (HRMS) were recorded on a SolariX 7.0 T mass spectrometer (Bruker, Germany).

Femtosecond transient absorption (fs-TA) experiments. The fs-TA measurements were conducted with an apparatus and methods detailed previously.[1] A femtosecond regenerative amplified Ti: sapphire laser system was employed for the fs-TA measurements, where the amplifier was seeded with 120 fs laser pulses from an oscillator. The laser probe pulse was generated by directing approximately 5% of the amplified 800 nm pulses through a CaF_2 crystal to produce a white-light continuum (350-800 nm). This probe beam was then split into two components before passing through the sample: one probe beam passed through the sample, while the other was directed to a reference spectrometer to monitor fluctuations in probe beam intensity. The AN–MI solution in acetonitrile (ACN) was excited at 266 nm (0.4 mW), whereas the DBAN–MI and AN–DBMI solutions in ACN were excited at 312 nm (0.3 mW).

Nanosecond transient absorption (ns-TA) Spectroscopy. The ns-TA spectra were recorded using an LP980 laser flash photolysis spectrometer (Edinburgh Instruments, UK). Signal digitization was performed with a Tektronix MDO 3022 oscilloscope. Prior to measurement, all samples were degassed with N_2 for approximately 15 min. Kinetic decay traces and fitting data were processed using L900 software.

Computational study. Time-dependent density functional theory (TD-DFT) calculations were performed using the Gaussian 16 program. [2-4] The B3LYP functional and 6-31G(d,p) basis set were employed to obtain the electron cloud distributions of the highest occupied molecular orbital (HOMO) and lowest unoccupied molecular orbital (LUMO), as well as the excitation energies and electrostatic potential distributions of the singlet (S_n) and triplet (T_n) states. Spin–orbit coupling (SOC) constants between the singlet and triplet states were calculated using the ORCA 4.2.1 package. The geometries of monomers and dimers used for theoretical calculations were extracted from the single-crystal structures.

Synthesis of AN–MI. A mixture of anthracene (AN, 1.50 g, 8.43 mmol) and maleimide (MI, 0.82 g, 8.43 mmol) was sealed in a pressure-resistant tube with toluene (15 mL) and heated at 150 °C for 24 h. After cooling to room temperature, a large amount of white solid precipitated. The crude product was purified by column chromatography using dichloromethane/acetone (20:1, v/v) as the eluent, followed by drying overnight in a vacuum oven at 50 °C to afford a white solid (0.81 g, yield 33%).^{1}H NMR (500 MHz, DMSO-d_6) δ 10.76 (s, 1H), 7.45 (m, J = 5.3, 3.3 Hz, 2H), 7.27 (m, J = 5.4, 3.3 Hz, 2H), 7.14 (m, J = 5.4, 4.2, 3.3 Hz, 4H), 4.73 (d, J = 17.8 Hz, 2H), 3.23–3.17 (m, 2H); ^{13}C NMR (126 MHz, DMSO-d_6) δ 178.48, 142.54, 139.94, 126.91, 126.65, 125.19, 124.62, 48.10, 44.91; HRMS ($C_{18}H_{13}NO_2$): m/z 298.0838 $[M + Na]^+$ (calcd 298.0838).

Synthesis of BAN–MI. 9-Bromoanthracene (BAN, 1.00 g, 3.89 mmol) and MI (0.38 g, 3.89 mmol) were reacted in toluene (10 mL) at 150 °C for 24 h in a sealed tube. A yellowish white solid formed upon cooling. The crude product was purified by column chromatography (dichloromethane/acetone = 12:1, v/v) and dried under vacuum at 50 °C overnight to yield a white solid (0.97 g, 73%). ^{1}H NMR (500 MHz, DMSO-d_6) δ 10.95 (s, 1H), 7.81–7.74 (m, 1H), 7.62–7.56 (m, 1H), 7.55–7.51 (m, 1H), 7.36–7.32 (m, 1H), 7.28 (m, J = 10.1, 5.6, 2.4 Hz, 4H), 4.84 (d, J = 3.3 Hz, 1H), 3.48 (d, J = 8.7 Hz, 1H), 3.36 (m, J = 8.7, 3.3 Hz, 1H); ^{13}C NMR (126 MHz, DMSO-d_6) δ 176.84, 175.03, 141.72, 141.21, 139.17, 138.30, 128.31, 128.11, 127.50, 127.14, 125.27, 125.20, 125.12, 124.32, 65.78, 54.60, 50.21, 44.42; HRMS ($C_{18}H_{12}BrNO_2$): m/z 375.9945 $[M + Na]^+$ (calcd 375.9944).

Synthesis of DBAN–MI. 9,10-Dibromoanthracene (DBAN, 1.50 g, 4.46 mmol) and MI (0.43 g, 4.46 mmol) were heated in toluene (10 mL) at 150 °C for 24 h in a sealed tube. The resulting white solid was purified by column chromatography using acetone as the eluent and dried in a vacuum oven at 50 °C overnight to give a white solid (0.78 g, 40%). ^{1}H NMR (500 MHz, DMSO-d_6) δ 11.14 (s, 1H), 7.86 (m, J = 7.6, 4.0 Hz, 2H), 7.66 (m, J = 7.7, 4.0 Hz, 2H), 7.42 (m, J = 15.2, 5.3, 3.4 Hz, 4H), 3.63 (s, 2H); ^{13}C NMR (126 MHz, DMSO-d_6) δ 173.43, 140.38, 137.49, 129.02, 128.73, 125.34, 125.18, 64.23, 56.25; HRMS ($C_{18}H_{11}Br_2NO_2$): m/z 455.9033 $[M + Na]^+$ (calcd 455.9028).

Synthesis of AN–BMI. Anthracene (AN, 0.50 g, 2.80 mmol) and 3-bromomaleimide (BMI, 0.49 g, 2.80 mmol) were mixed with toluene (15 mL) in a sealed tube and heated at 150 °C for 24 h. A yellowish white solid was obtained upon cooling. The crude product was purified by column chromatography (dichloromethane/acetone = 20:1, v/v) and dried in vacuo at 50 °C overnight to afford a white solid (0.36 g, 34%). ^{1}H NMR (500 MHz, DMSO-d_6) δ 11.49 (s, 1H), 7.52 (m, J = 8.9, 6.3, 3.7 Hz, 2H), 7.31 (m, J = 12.2, 5.5, 2.8 Hz, 2H), 7.27–7.16 (m, 4H), 4.92 (s, 1H), 4.81 (d, J = 3.5 Hz, 1H), 3.49 (d, J = 3.5 Hz, 1H); ^{13}C NMR (126 MHz, DMSO-d_6) δ 175.02, 174.76, 140.63, 140.14, 139.13, 138.30, 127.95, 127.55, 127.45, 126.84, 126.23, 125.42, 124.97, 61.53, 58.05, 52.21, 45.35; HRMS ($C_{18}H_{12}BrNO_2$): m/z 375.9952 $[M + Na]^+$ (calcd 375.9944).

Synthesis of AN–DBMI. Anthracene (AN, 0.70 g, 3.93 mmol) and 3,4-dibromomaleimide (DBMI, 1.00 g, 3.92 mmol) were reacted in toluene (10 mL) at 150 °C for 24 h in a sealed tube. After cooling, a yellowish white solid formed. The crude product was purified by column chromatography using chloroform as the eluent, followed by drying under vacuum at 50 °C overnight to yield a white solid (0.44 g, 26%). ^{1}H NMR (500 MHz, DMSO-d_6) δ 12.10 (s, 1H), 7.54 (m, J = 5.3, 3.3 Hz, 2H), 7.36 (m, J = 5.4, 3.3 Hz, 2H), 7.29 (m, J = 5.4, 3.2 Hz, 2H), 7.24 (m, J = 5.4, 3.2 Hz, 2H), 5.09 (s, 2H); ^{13}C NMR (126 MHz, DMSO-d_6) δ 172.69, 138.61, 138.02, 128.44, 127.50, 127.09, 126.17, 67.87, 53.83; HRMS ($C_{18}H_{11}Br_2NO_2$): m/z 455.9031 $[M + Na]^+$ (calcd 455.9028).

Single-crystal cultivation. Single crystals of AN–MI, BAN–MI, and AN–BMI were obtained by slow evaporation of their acetone solutions, while those of DBAN–MI and AN–DBMI were grown by slow evaporation from chloroform solutions at room temperature.

Supplementary Figures and Tables

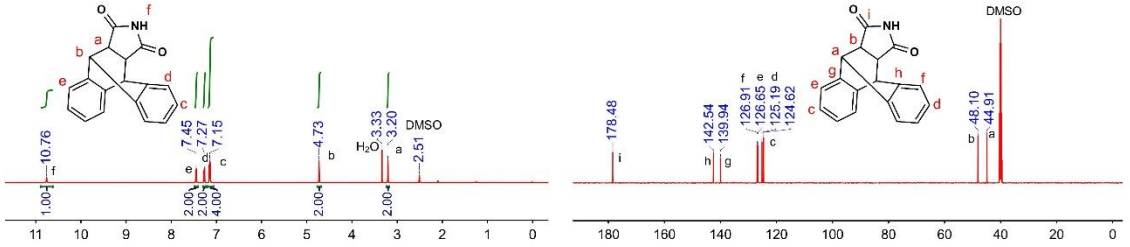

Fig. S1 ^{1}H and ^{13}C NMR spectra of AN–MI.

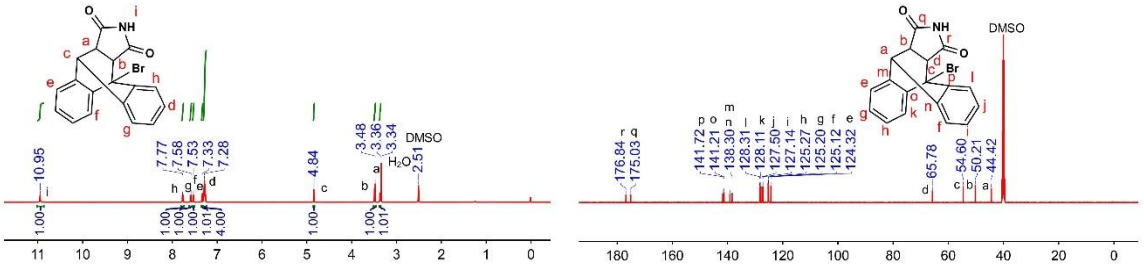

Fig. S2 ^{1}H and ^{13}C NMR spectra of BAN–MI.

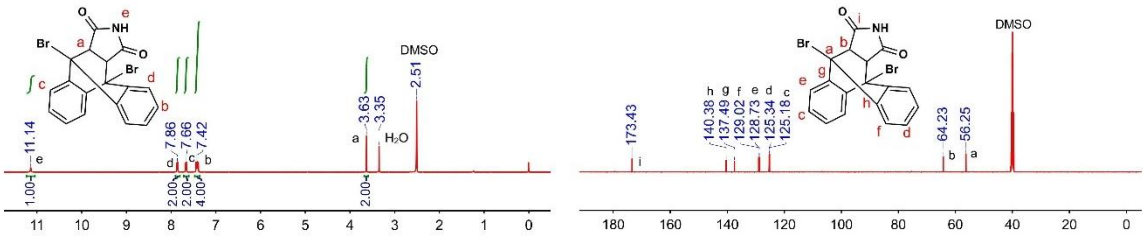

Fig. S3 ^{1}H and ^{13}C NMR spectra of DBAN–MI.

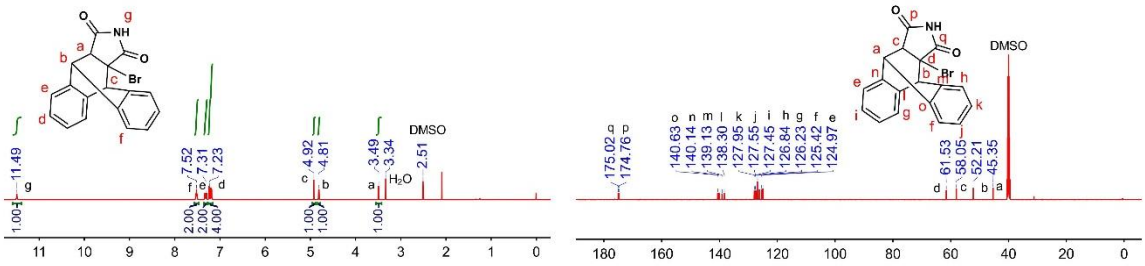

Fig. S4 ^{1}H and ^{13}C NMR spectra of AN–BMI.

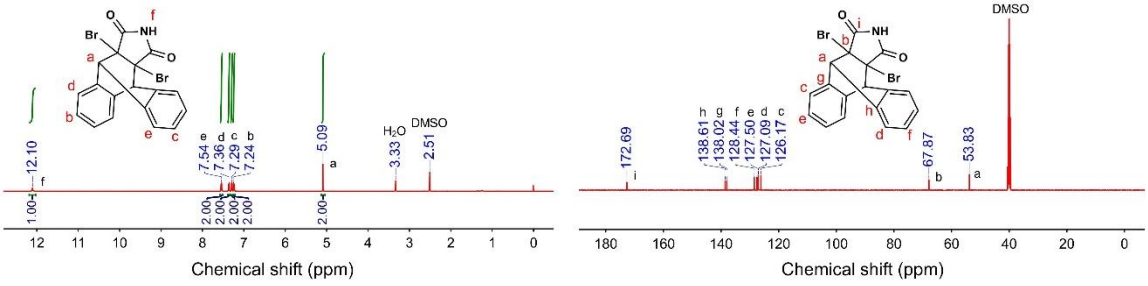

Fig. S5 ^{1}H and ^{13}C NMR spectra of AN–DBMI.

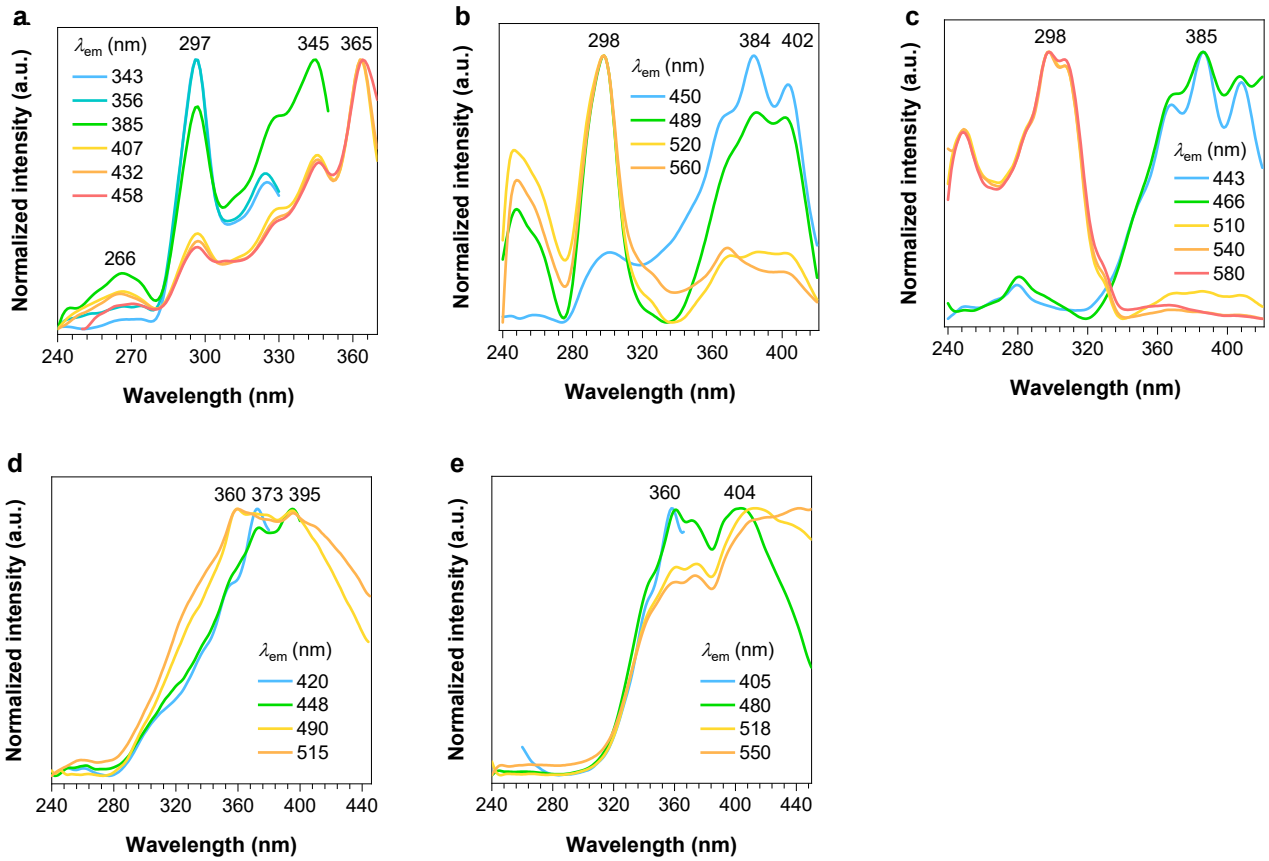

Fig. S6 Excitation spectra with different λ_{em}s of (A) AN–MI, (B) BAN–MI, (C) DBAN–MI, (D) AN–BMI, and (E) AN–DBMI.

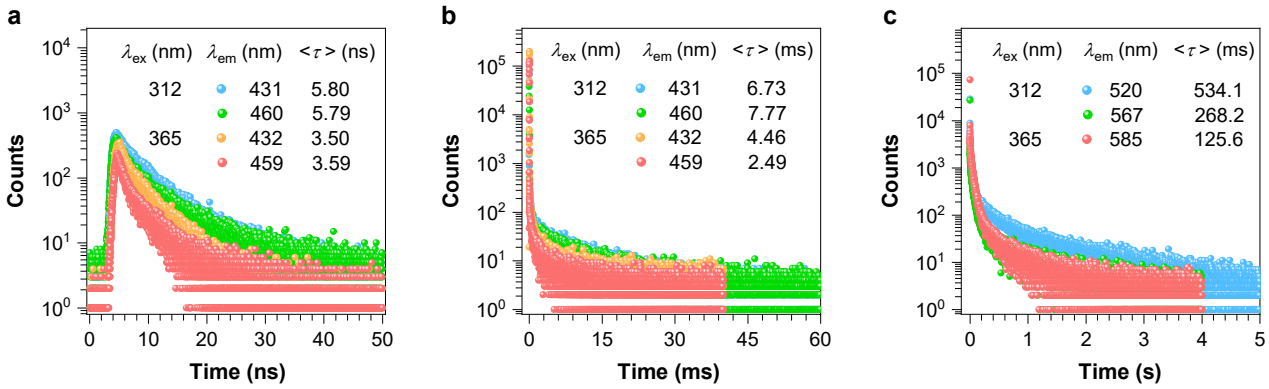

Fig. S7 (a) Nanosecond and (b) (c) microsecond scale lifetime profiles under 312 and 365 nm of AN–MI crystals.

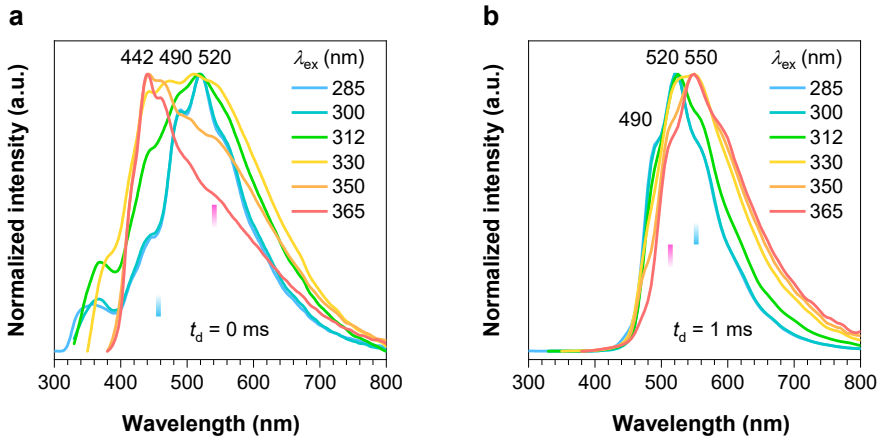

Fig. S8 (a) Prompt (t_d = 0 ms) and (b) delayed (t_d = 1 ms) emission spectra with different λ_{ex}s of BAN–MI crystals.

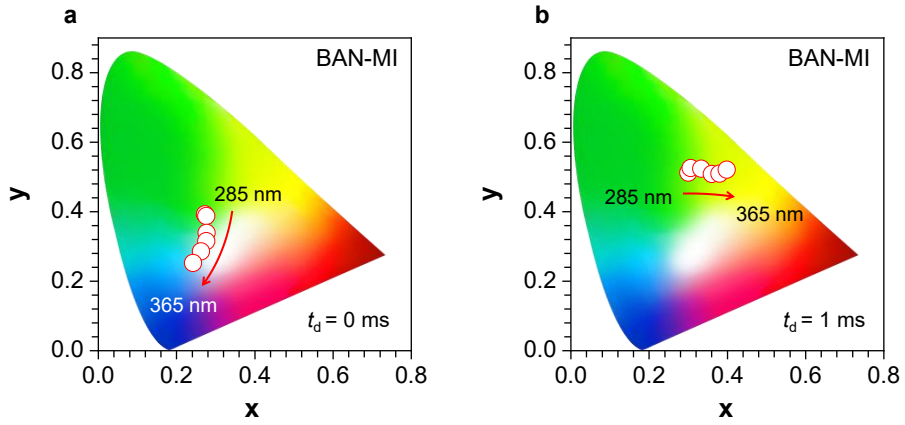

Fig. S9 CIE coordinate diagrams of (a) prompt (t_d = 0 ms) emission and (b) delayed (t_d = 1 ms) emission with different λ_{ex}s of BAN–MI crystals.

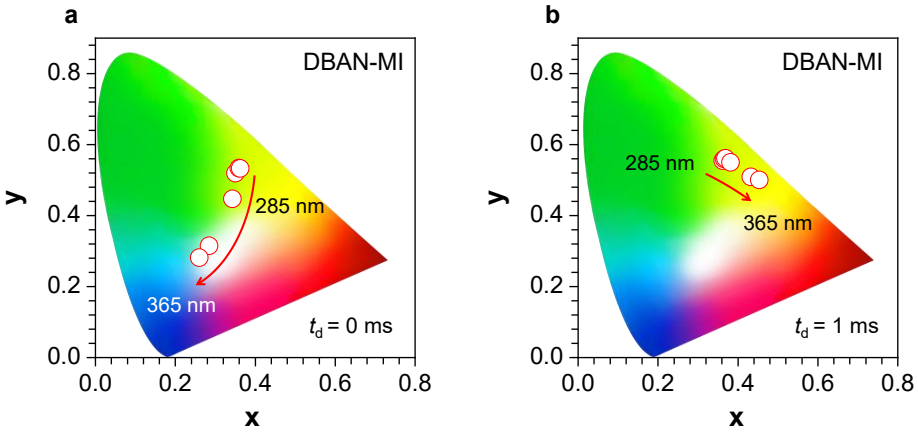

Fig. S10 CIE coordinate diagrams of (a) prompt (t_d = 0 ms) emission and (b) delayed (t_d = 1 ms) emission with different λ_{ex}s of DBAN–MI crystals.

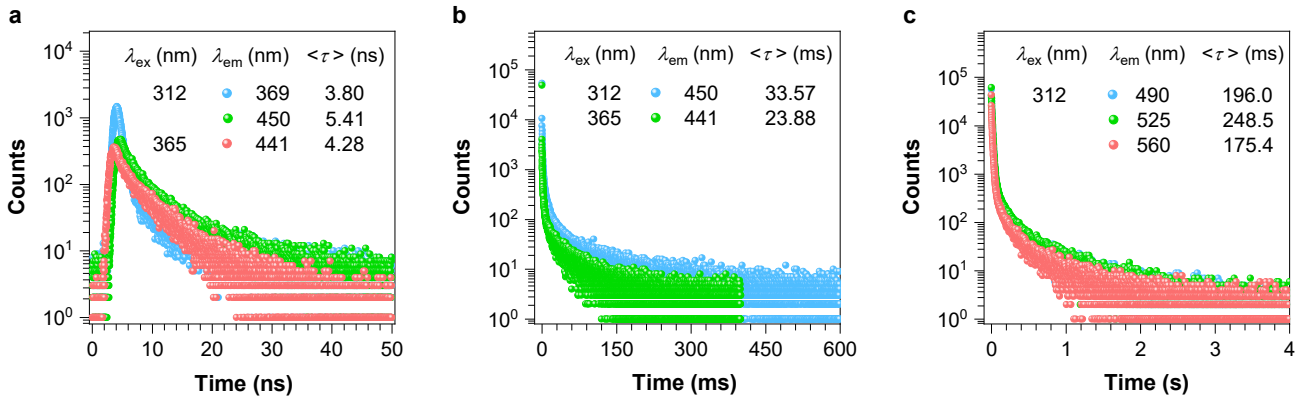

Fig. S11 (a) Nanosecond and (b) (c) microsecond scale lifetime profiles under 312 and 365 nm of BAN–MI crystals.

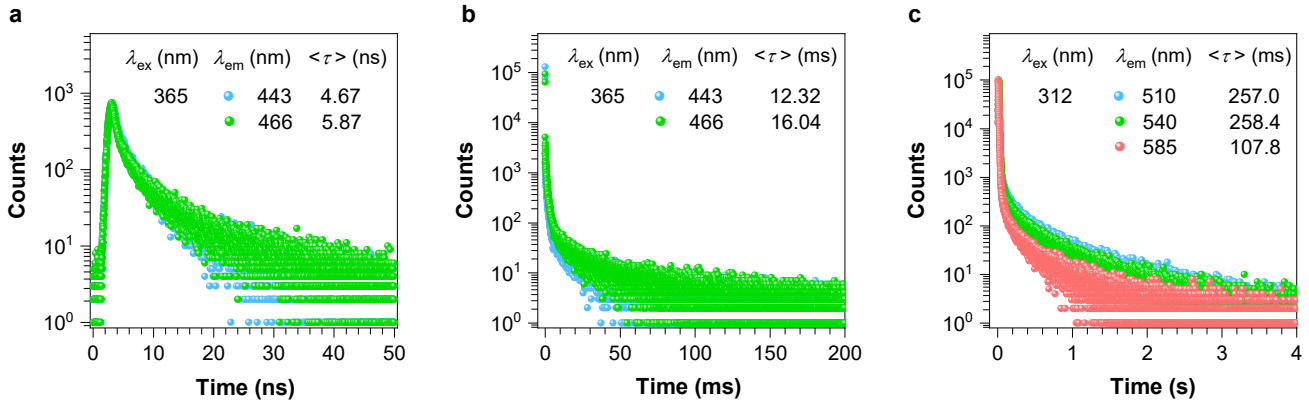

Fig. S12 (a) Nanosecond and (b) (c) microsecond scale lifetime profiles under 312 and 365 nm of DBAN–MI crystals.

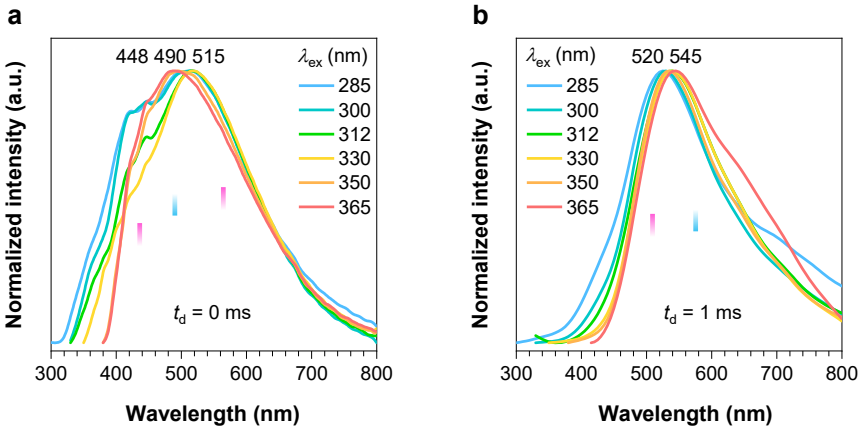

Fig. S13 (a) Prompt (t_d = 0 ms) and (b) delayed (t_d = 1 ms) emission spectra with different λ_{ex}s of AN–BMI crystals.

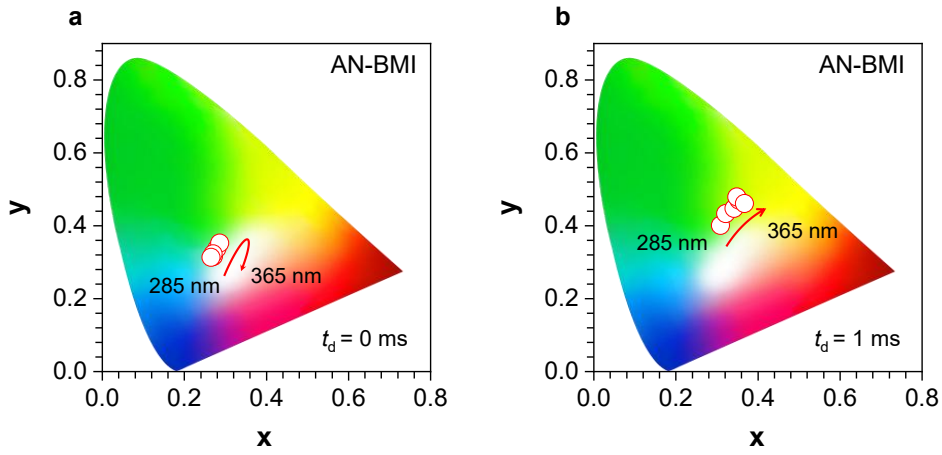

Fig. S14 CIE coordinate diagrams of (a) prompt (t_d = 0 ms) emission and (b) delayed (t_d = 1 ms) emission with different λ_{ex}s of AN–BMI crystals.

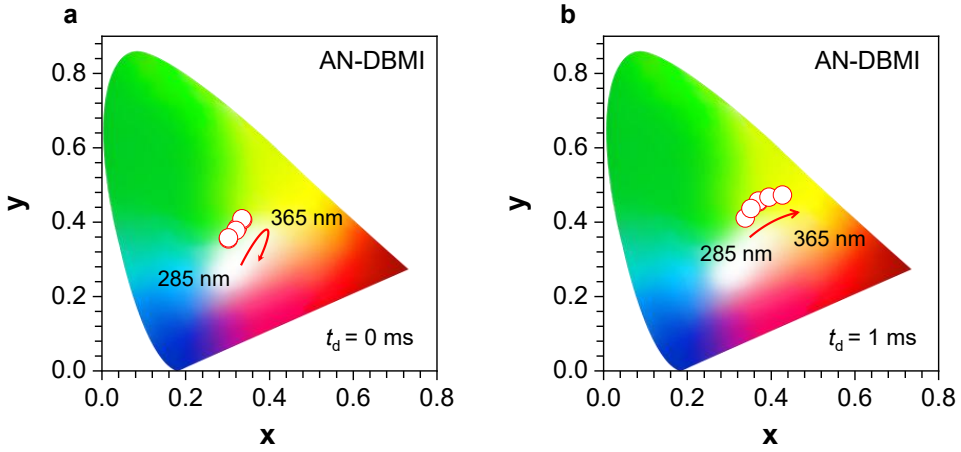

Fig. S15 CIE coordinate diagrams of (a) prompt (t_d = 0 ms) emission and (b) delayed (t_d = 1 ms) emission with different λ_{ex}s of AN–DBMI crystals.

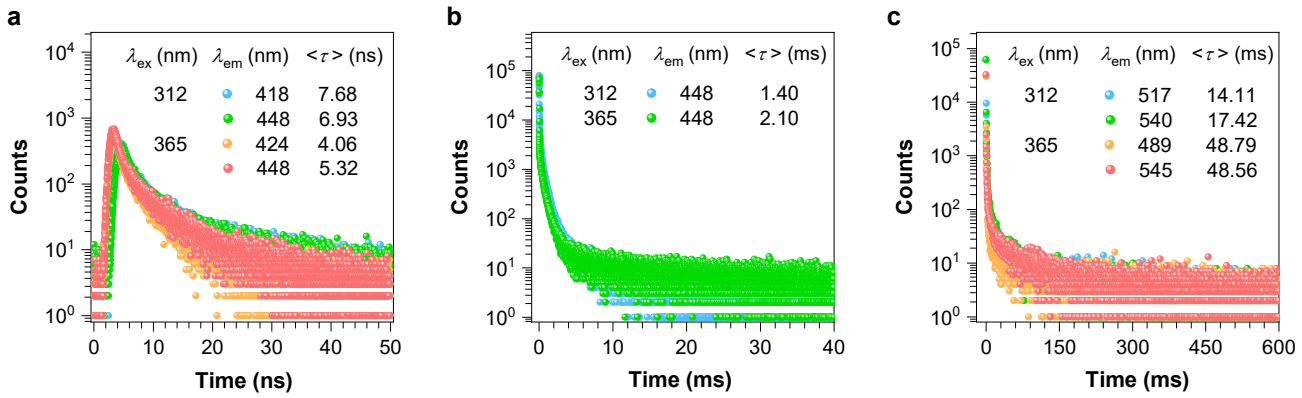

Fig. S16 (a) Prompt (t_d = 0 ms) and (b) delayed (t_d = 1 ms) emission spectra with different λ_{ex}s of AN–BMI crystals.

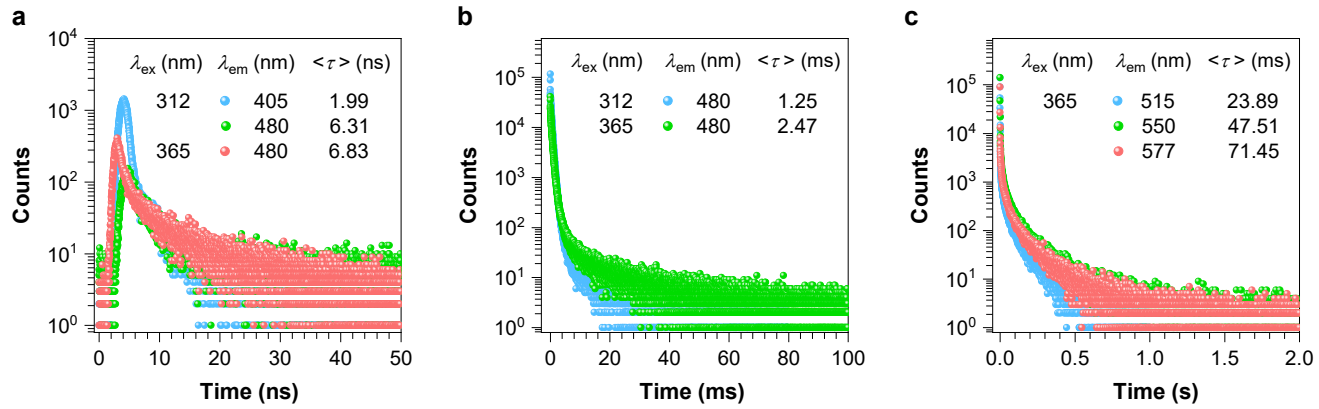

Fig. S17 (a) Prompt (t_d = 0 ms) and (b) delayed (t_d = 1 ms) emission spectra with different λ_{ex}s of AN–DBMI crystals.

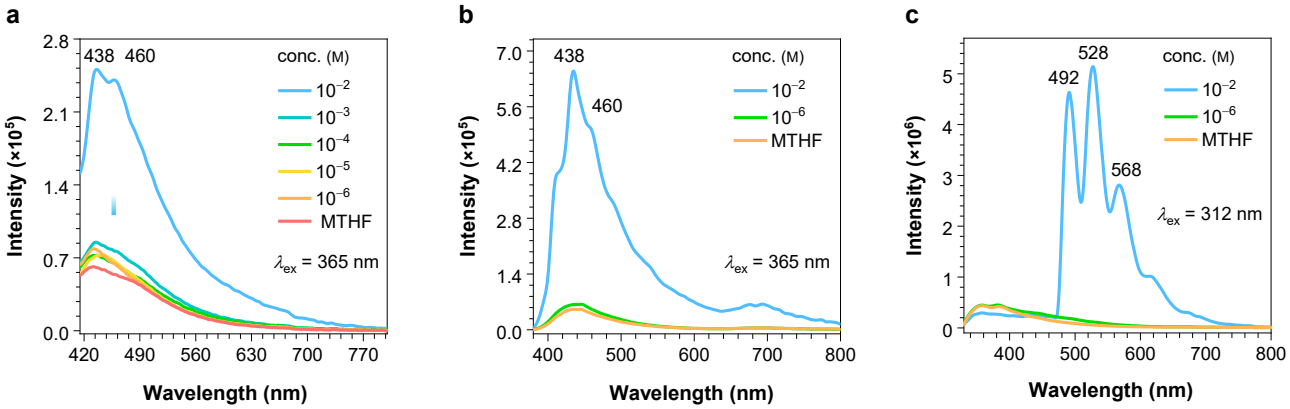

Fig. S18 (a) Emission spectra (λ_{ex} = 365 nm) of different of DBAN–MI/MTHF solutions at room temperature. Emission spectra of 10^{-2} and 10^{-6} M DBAN–MI/MTHF solutions and MTHF under (b) 365 and (c) 312 nm excitation at 77 K.

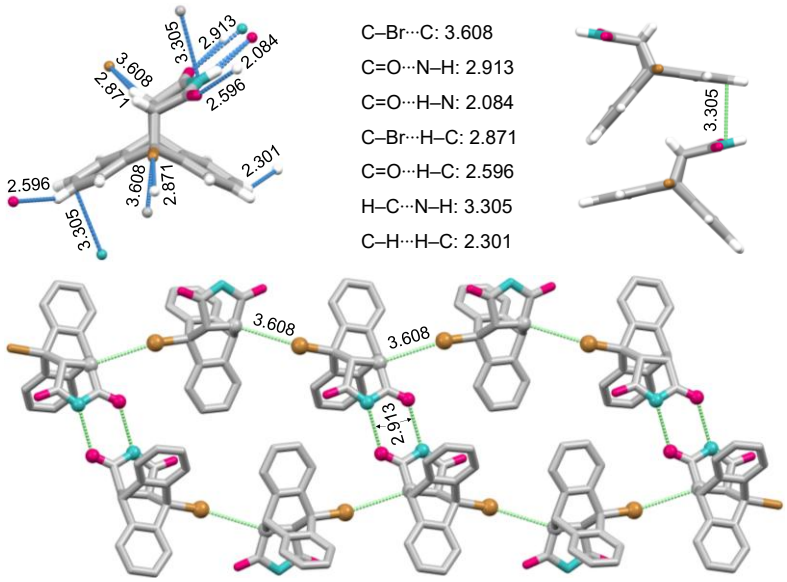

Fig. S19 Single crystal structure and intermolecular stacking analysis of BAN–MI.

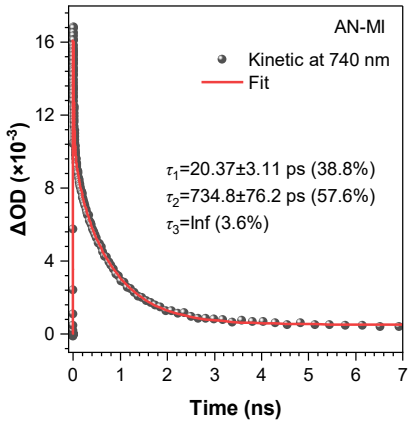

Fig. S20 The fs-TA spectra decay curve in 740 nm of AN–MI in ACN.

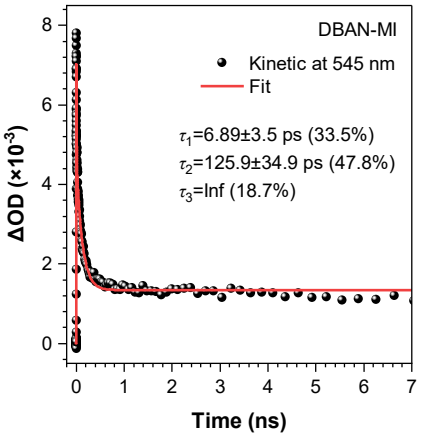

Fig. S21 The fs-TA spectra decay curve in 545 nm of DBAN–MI in ACN.

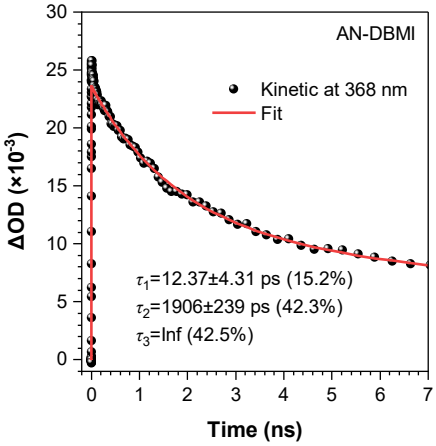

Fig. S22 The fs-TA spectra decay curve in 368 nm of AN–DBMI in ACN.

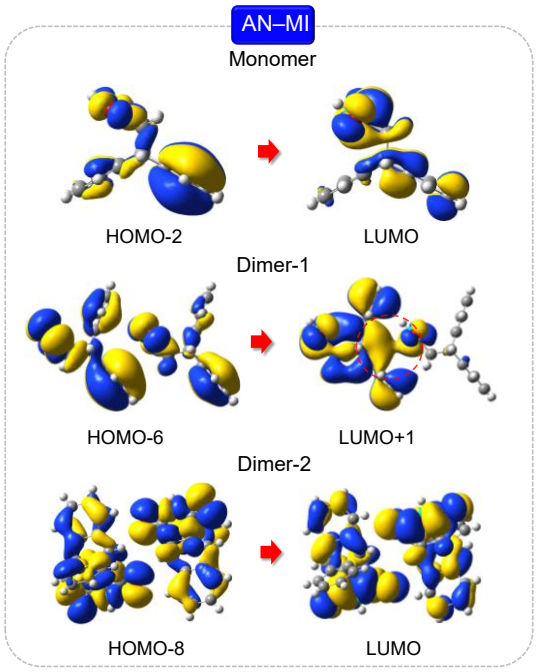

Fig. S23 Related energy levels electron densities of the selected monomers and dimers of AN–MI.

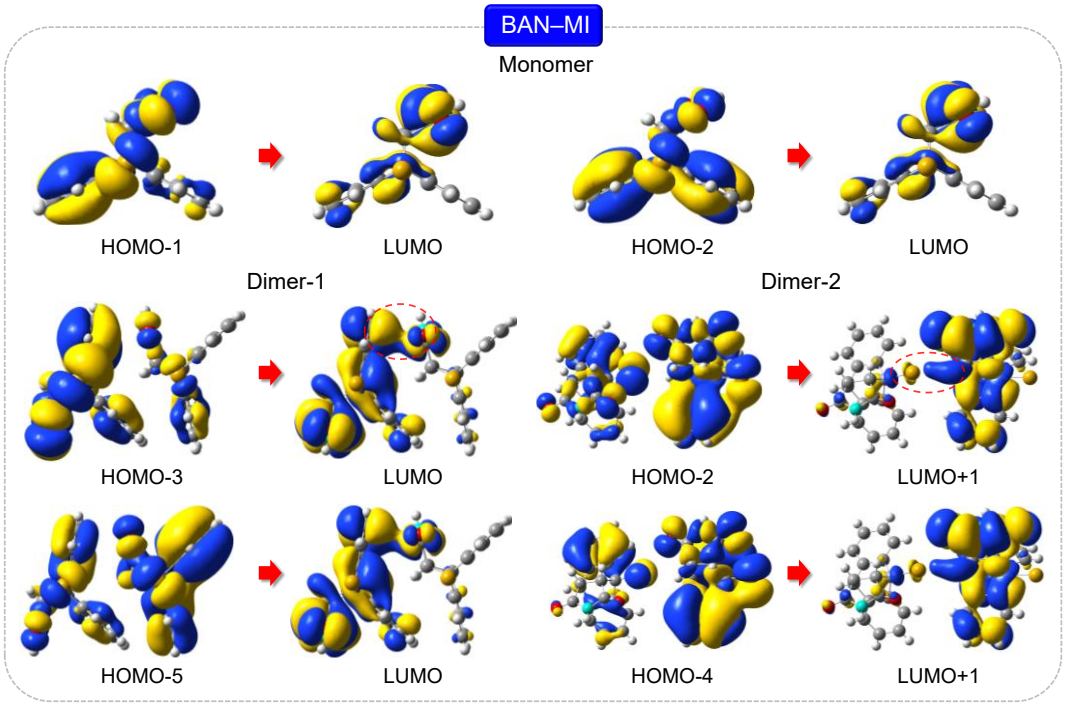

Fig. S24 HOMO, LUMO, and other related energy levels electron densities of the selected monomers and dimers of BAN–MI.

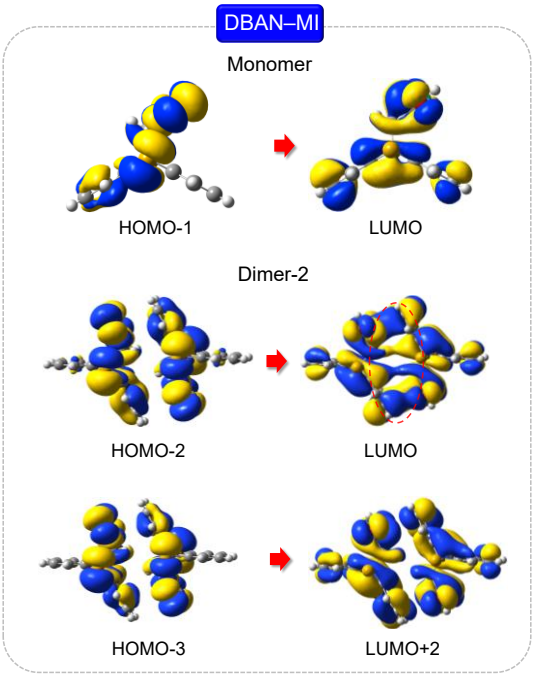

Fig. S25 Related energy levels electron densities of the selected monomers and dimers of DBAN–MI.

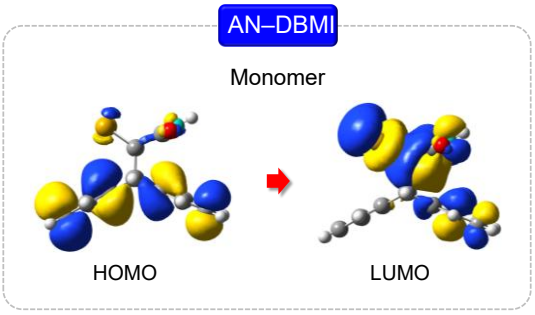

Fig. S26 HOMO and LUMO energy levels electron densities of the monomer of AN–DBMI.

Table S1. Room-temperature fluorescence lifetime of AN–MI.

λ_{ex} (nm)	λ_{em} (nm)	A_1 (%)	τ_1 (ns)	A_2 (%)	τ_2 (ns)	A_3 (%)	τ_3 (ns)	τ (ns)
312	343	34.28	0.49	19.11	3.94	46.62	8.21	4.75
	356	11.41	0.52	14.64	3.09	73.95	8.02	6.44
	385	3.80	0.97	66.38	4.58	29.82	10.69	6.26
	407	1.72	0.61	59.23	3.92	39.05	8.02	5.46
365	385	51.72	0.25	48.28	3.44	-	-	1.79
	407	7.57	0.60	92.43	3.76	-	-	3.52

Table S2. Room-temperature phosphorescence lifetime of AN–MI, BAN–MI, DBAN–MI, and AN–DBMI.

λ_{ex} (nm)	λ_{em} (nm)	A_1 (%)	τ_1 (ms)	A_2 (%)	τ_2 (ms)	A_3 (%)	τ_3 (ms)	A_4 (%)	τ_4 (ms)	τ (ms)
AN–MI										
285	505	24.38	4.44	36.81	9.21	8.61	222.52	30.20	1497.4	475.85
312	520	18.53	5.86	17.09	27.89	24.92	213.44	39.45	1204.1	534.07
	567	10.76	4.62	41.99	35.43	18.94	137.64	28.31	800.96	268.19
365	585	5.58	1.66	24.11	20.44	51.46	58.58	18.85	479.94	125.63
BAN–MI										
285	490	18.84	13.71	23.57	119.74	57.59	541.97	-	-	342.93
	520	7.34	14.33	10.33	73.62	23.78	200.43	58.55	580.57	396.24
	560	6.13	8.99	11.36	21.87	25.82	132.93	56.69	527.67	336.49
312	490	33.36	14.32	34.11	101.01	32.52	481.91	-	-	195.95
	525	13.92	12.85	12.64	33.95	36.89	128.23	36.56	533.54	248.45
	560	32.60	14.33	35.53	100.80	31.88	423.04	-	-	175.35
365	515	27.46	14.96	49.04	83.96	23.50	289.60	-	-	113.34
	545	15.10	3.27	52.82	12.77	21.13	72.69	10.95	280.07	53.27
	595	19.82	2.74	47.94	10.98	20.39	51.76	11.85	206.92	40.88
DBAN–MI										
285	510	7.93	6.39	21.55	67.30	29.07	196.57	41.45	725.14	372.72
	540	11.02	6.25	20.56	62.17	28.77	192.95	39.66	693.98	344.21
	585	12.63	5.97	14.27	44.31	32.54	146.99	40.56	628.39	309.78
312	510	25.91	5.72	12.23	31.73	25.01	145.50	36.85	584.20	257.03
	540	19.10	6.03	14.89	36.19	26.38	145.75	39.63	538.60	258.44
	585	53.35	5.78	19.55	52.36	27.11	348.64	-	-	107.84

365	560	20.34	4.82	17.33	22.83	49.30	85.83	13.02	338.98	91.39
	590	39.62	3.39	18.14	11.18	33.78	73.28	8.46	272.16	51.15
					AN–BMI					
285	515	25.98	0.13	56.23	0.66	8.40	6.90	9.38	74.44	7.97
	525	27.42	0.11	52.19	0.65	10.67	5.94	9.73	65.71	7.40
312	517	70.51	0.61	14.85	7.13	14.64	86.20	-	-	14.11
	540	60.82	0.60	19.19	7.34	19.99	78.29	-	-	17.42
365	489	60.73	0.60	11.29	9.69	27.98	169.16	-	-	48.79
	545	41.22	0.72	22.99	12.35	35.79	126.92	-	-	48.56
					AN–DBMI					
285	518	21.37	0.59	16.01	2.43	26.74	12.36	35.88	58.57	24.84
	550	13.17	1.00	33.21	7.77	53.61	47.29	-	-	28.06
312	518	33.36	0.56	14.17	3.01	24.66	22.37	27.81	114.64	38.01
	550	61.72	0.39	13.01	1.53	11.77	15.85	13.50	100.69	15.90
365	515	51.21	0.46	14.07	2.08	17.23	19.64	17.49	114.21	23.89
	550	31.27	0.59	17.24	5.55	29.81	34.80	21.68	166.01	47.51
	577	9.46	2.40	23.74	12.40	35.63	44.50	31.17	168.18	71.45

Table S3. Photophysical data of AN–MI, BAN–MI, DBAN–MI, AN–BMI, and AN–DBMI.[a]

Sample	λ_p (nm)	τ_p (ms)	Φ_c (%)	Φ_f (%)	Φ_p (%)	k_r^p (s^{-1})	k_{nr}^p (s^{-1})
AN–MI	510	534.07	16.85	13.28	3.57	0.07	1.81
BAN–MI	525	248.45	15.82	2.42	13.40	0.54	3.49
DBAN–MI	540	258.44	21.49	0.00	21.49	0.83	3.04
AN–BMI	540	48.56	5.01	0.74	4.26	0.88	19.72
AN–DBMI	550	47.51	4.31	0.33	3.98	0.84	20.21

[a] $\Phi_c = \Phi_f + \Phi_p$; $k_r^p = \Phi_p / \tau_p$; $k_{nr}^p = (1-\Phi_p)/\tau_p$.

Table S4. Single crystal information and parameters of AN–MI, BAN–MI, DBAN–MI, and AN–DBMI.

	AN–MI	BAN–MI	DBAN–MI	AN–DBMI
Formula	$C_{18}H_{13}NO_2$	$C_{18}H_{12}BrNO_2$	$C_{18}H_{11}Br_2NO_2$	$C_{18}H_{11}Br_2NO_2$
Formula Weight	275.29	354.20	433.10	433.10
Meas. Temp. (K)	273	298	297	298
Wavelength (Å)	1.54178	1.54178	1.54178	1.54178
Space Group	P21/m	P21/n	P21/c	P21/c
Cell Length (Å)	a = 6.8308 (5) b = 12.1154 (10) c = 8.1913 (8)	a = 8.011 (3) b = 17.559 (4) c = 10.817 (4)	a = 11.6008 (5) b = 9.0559 (3) c = 15.4692 (5)	a = 12.654 (3) b = 7.375 (2) c = 17.626 (5)
Cell Angle (°)	α = 90 β = 105.093 (4) γ = 90	α =90 β = 105.964(14) γ = 90	α = 90 β = 109.994 (2) γ = 90	α = 90 β = 104.48 (2) γ = 90
Cell Volume (Å^3)	654.51 (10)	1462.9 (8)	1527.18 (10)	1592.7(8)
Z	2	4	4	4
Density (g cm^{-3})	1.397	1.608	1.884	1.806
F (000)	288.0	712.0	848.0	848.0
h_{max}, k_{max}, l_{max}	8, 14, 9	9, 20, 13	13, 10, 18	15, 8, 21
T_{min}, T_{max}	0.650, 0.753	0.601, 0.753	0.602, 0.753	0.432, 0.457

Table S5. Theoretical calculation results of AN–MI.

Aggregation state	Excited state	Excitation energy (eV)	Transition configuration (%)
Monomer	S_1	4.9040	**H-5→ L+5 (12.450); H-4→ L (49.199); H-2→ L (32.334); H-1→ L (26.548)**
	T_1	3.7424	H-2→ L+2 (25.640); H-1→ L+3 (20.322); H→ L (22.526); H→ L+1 (44.758)
	T_2	3.8513	H-2→ L+2 (19.589); H-2→ L+3 (21.751); H-1→ L+2 (25.061); H→ L (12.748); H→ L+4 (34.783)
	T_3	4.4164	**H-5→ L+5 (17.208); H-4→ L (49.109); H-2→ L (31.295); H-1→ L (23.524)**
	T_4	4.5656	H-2→ L+1 (15.348); H→ L+2 (60.040)
	T_5	4.6260	H-3→ L+4 (12.221); H-2→ L+2 (37.137); H-2→ L+3

			(13.357); H-1→ L+3 (24.283)
	T_6	4.7131	**H-2→ L (10.653);** H-2→ L+1 (10.231); H-2→ L+4 (14.452); H-1→ L+1 (27.498); H→ L+3 (43.058)
	T_7	4.7364	H-3→ L (15.397); H-3→ L+1 (27.695); H-2→ L+2 (23.478); H-2→ L+3 (21.041); H-1→ L+2 (29.281); H→ L+1 (10.191)
	T_8	4.9033	H-5→ L (48.822); H-4→ L+5 (24.919); H-3→ L+1 (13.792); H-2→ L+5 (13.556); H-1→ L+5 (10.865); H→ L (21.857)
Dimer-1	S_1	4.8423	**H-11→ L+10 (12.199); H-6→ L (38.625); H-6→ L+1 (27.094); H-5→ L (15.743); H-5→ L+1 (11.367)**
	T_1	3.7451	H-4→ L+9 (24.892); H-3→ L+5 (29.328); H-2→ L+8 (19.528); H→ L+3 (34.832)
	T_2	3.7648	H-9→ L+6 (14.333); H-8→ L+7 (24.382); H-7→ L+2 (23.025); H-6→ L+6 (13.176); H-5→ L+2 (16.094); H-5→ L+6 (13.746); H-1→ L (34.532)
	T_3	3.8512	H-5→ L+5 (19.842); H-4→ L+4 (25.547); H→ L+3 (11.226)
	T_4	3.8718	H-8→ L+1 (25.357)
	T_5	4.4111	**H-11→ L+10 (16.832); H-6→ L (36.874); H-6→ L+1 (26.264); H-5→ L (13.915); H-5→ L+1 (10.669)**
	T_6	4.4280	H-10→ L+11 (16.837); H-2→ L+1 (12.940); H-2→ L+3 (34.023); H-2→ L+4 (26.398)
	T_7	4.5608	H-4→ L+8 (24.202); H-3→ L+3 (12.435); H→ L+5 (60.071)
	T_8	4.5920	H-8→ L+6 (22.453); H-7→ L (11.277); H-1→ L+2 (58.392)
	T_9	4.6283	H-7→ L+8 (10.610); H-5→ L+5 (14.030); H-3→ L+5 (40.986); H-2→ L+5 (12.918); H-2→ L+8 (23.786); H→ L+4 (26.977)
	T_{10}	4.6319	H-9→ L+2 (15.479); H-8→ L+7 (11.833); H-6→ L+2 (18.448); H-1→ L (29.354)
Dimer-2	S_1	4.7204	**H-8→ L (41.287); H-5→ L+1 (15.594); H-3→ L (16.357); H→ L+1 (12.685)**
	T_1	3.7408	H-7→ L+8 (12.982); H-7→ L+9 (12.899); H-1→ L+3 (22.328); H→ L+3 (24.899)

	T_2	3.7410	H-7→ L+9 (12.091); H-6→ L+9 (12.842); H-5→ L+5 (11.904); H-4→ L+4 (11.458); H-3→ L+4 (11.260); H-2→ L+5 (11.810); H-1→ L+2 (25.008); H-1→ L+3 (25.212)
	T_3	3.8503	H-7→ L+2 (18.913); H-6→ L+3 (17.540)
	T_4	3.8504	H-5→ L+5 (14.573); H-4→ L+4 (13.664); H-3→ L+5 (10.109); H-3→ L+6 (11.617); H-2→ L+7 (11.922); H-1→ L+8 (18.194); H→ L+9 (16.036)
	T_5	4.4315	**H-8→ L (42.699); H-5→ L+1 (13.378); H-3→ L (14.906)**
	T_6	4.4317	H-11→ L+10 (11.354); H-10→ L+11 (10.968); H-8→ L+1 (42.814); H-5→ L (13.415); H-3→ L+1 (14.814)
	T_7	4.5736	H-6→ L+7 (12.504); H-1→ L+4 (32.056); H-1→ L+5 (21.959); H→ L+4 (27.808); H→ L+5 (32.982)
	T_8	4.5737	H-6→ L+6 (13.087); H-1→ L+5 (34.987); H→ L+4 (30.305)
	T_9	4.6204	H-5→ L+4 (15.410); H-5→ L+5 (13.658); H-4→ L+4 (14.035); H-4→ L+5 (14.467); H-3→ L+4 (17.165); H-3→ L+5 (17.016); H-2→ L+4 (19.381); H-2→ L+5 (16.561); H-1→ L+3 (17.721); H→ L+3 (18.276)
	T_{10}	4.6206	H-5→ L+4 (12.694); H-4→ L+5 (15.113); H-3→ L+5 (17.652); H-3→ L+6 (11.921); H-2→ L+4 (16.064); H-2→ L+7 (12.259); H-1→ L+2 (19.592); H-1→ L+3 (18.525)

[a]All triplet states (T_n) with orbital transition characteristics matching those of S_1 are highlighted in bold.

Table S6. Theoretical calculation results of BAN–MI.

Aggregation state	Excited state	Excitation energy (eV)	Transition configuration (%)
Monomer	S_1	4.6900	**H-7→ L+6 (10.146); H-6→ L (16.390); H-4→ L (11.136); H-2→ L (28.656); H-1→ L (54.351)**
	T_1	3.7612	H-4→ L+1 (10.515); H-4→ L+4 (17.157); H-3→ L+3 (13.903); H-2→ L+1 (27.016); H-1→ L+2 (19.862); H-1→ L+3 (15.469); H→ L+1 (14.650); H→ L+2 (30.097)
	T_2	3.8819	H-3→ L+1 (11.770); H-3→ L+3 (25.769); H-2→ L+3 (22.879); H→ L+1 (25.414); H→ L+2 (18.190)

	T_3	4.2136	**H-7→ L+6 (14.346); H-6→ L (19.135); H-4→ L (12.346); H-2→ L (27.374); H-1→ L (51.522)**
	T_4	4.6410	H-4→ L+1 (11.749); H-4→ L+4 (14.527); H-2→ L+2 (22.012); H→ L+1 (48.228); H→ L+4 (10.593)
	T_5	4.6502	H-4→ L+2 (15.473); H-4→ L+3 (19.365); H-1→ L+1 (18.785); H→ L+2 (42.481)
Dimer-1	S_1	4.6813	**H-5→ L (11.946); H-4→ L (10.995); H-3→ L (54.909)**
	T_1	3.7550	H-6→ L+2 (13.083); H-5→ L+7 (12.098); H-4→ L+3 (15.735); H-4→ L+4 (29.254); H-1→ L+1 (12.499); H-1→ L+5 (11.417)
	T_2	3.7653	H-6→ L+2 (35.198); H-6→ L+3 (10.030); H-3→ L+2 (17.848); H-1→ L (12.658); H-1→ L+4 (19.615); H→ L+5 (10.422)
	T_3	3.8789	H-6→ L+6 (10.411); H-5→ L+4 (14.302); H-4→ L+7 (16.624); H-1→ L+8 (10.920); H→ L+5 (27.273); H→ L+10 (13.965)
	T_4	3.8859	H-9→ L+2 (14.795); H-7→ L+2 (16.127); H-7→ L+6 (18.969); H-5→ L+4 (12.117); H-4→ L+7 (11.278); H-3→ L+2 (10.438); H-1→ L+3 (13.545); H→ L+5 (13.050)
	T_5	4.2063	**H-5→ L (11.365); H-4→ L (10.312); H-3→ L (51.964)**
	T_6	4.2346	H-12→ L+1 (15.214); H-2→ L (12.966); H-2→ L+1 (45.344); H-2→ L+3 (24.019)
	T_7	4.6305	H-8→ L+3 (15.152); H-8→ L+4 (12.651); H-8→ L+7 (11.500); H-5→ L+7 (13.408); H→ L+3 (31.120); H→ L+4 (39.380)
	T_8	4.6331	H-9→ L+2 (12.045); H-7→ L+6 (13.147); H-6→ L (10.955); H-4→ L+2 (19.530); H-2→ L+2 (18.684); H-1→ L+2 (39.729); H→ L+2 (10.374); H→ L+3 (10.524); H→ L+4 (16.216)
	T_9	4.6363	H-6→ L+2 (32.419); H-3→ L+2 (10.829); H-1→ L+3 (22.172)
	T_{10}	4.6434	H-8→ L+1 (10.501); H-8→ L+5 (10.673); H-5→ L+7 (16.657); H-4→ L+3 (19.717); H-4→ L+4 (20.259); H→ L+1 (21.617); H→ L+3 (12.591); H→ L+5 (32.037)
Dimer-2	S_1	4.6800	**H-12→ L+1 (14.581); H-8→ L+1 (12.010); H-4→ L+1 (34.696); H-2→ L+1 (48.525)**
	T_1	3.7560	H-8→ L+10 (16.320); H-4→ L+4 (21.970); H-3→ L+5 (13.054); H-2→ L+5 (20.702); H-2→ L+8 (11.199); H→ L+4 (14.351); H→ L+5 (30.780); H→ L+10 (10.287)

T_2	3.7610	H-9→ L+9 (17.198); H-4→ L+3 (11.312); H-3→ L+3 (29.239); H-3→ L+6 (19.738); H-1→ L (13.287); H-1→ L+9 (14.459)
T_3	3.8808	H-9→ L+2 (30.844); H-7→ L+3 (28.981); H-7→ L+7 (12.770); H-5→ L+6 (11.709)
T_4	3.8812	H-6→ L+8 (16.338); H-4→ L+8 (11.986); H→ L+4 (26.073); H→ L+5 (16.603)
T_5	4.2112	H-14→ L+13 (12.005); H-13→ L+1 (10.114); **H-12→ L+1 (16.956); H-8→ L+1 (13.148); H-4→ L+1 (33.283); H-2→ L+1 (45.592)**
T_6	4.2142	H-15→ L+12 (11.948); H-5→ L (43.825); H-3→ L (33.433)
T_7	4.6357	H-8→ L+4 (12.615); H-8→ L+10 (13.951); H-6→ L+7 (16.063); H-4→ L+5 (18.788); H→ L+4 (49.716); H→ L+10 (10.995)
T_8	4.6384	H-7→ L+3 (17.226); H-7→ L+7 (10.086); H-3→ L+3 (18.706); H-3→ L+6 (10.001); H-1→ L+2 (41.460)
T_9	4.6425	H-8→ L+5 (15.149); H-8→ L+8 (12.255); H-3→ L+4 (12.180); H-2→ L+4 (20.324); H→ L+5 (42.669)
T_{10}	4.6556	H-9→ L+6 (17.575); H-5→ L+2 (14.710); H-3→ L+3 (11.512); H-3→ L+9 (12.857); H-1→ L+3 (48.361)

[a]All triplet states (T_n) with orbital transition characteristics matching those of S_1 are highlighted in bold.

Table S7. Theoretical calculation results of DBAN–MI.

Aggregation state	Excited state	Excitation energy (eV)	Transition configuration (%)
Monomer	S_1	4.6588	**H-8→ L+1 (10.665); H-1→ L (52.929)**
	T_1	3.6737	H-5→ L+5 (11.092); H-4→ L+5 (21.856); H-2→ L+2 (31.702); H→ L (35.975); H→ L+1 (33.904)
	T_2	3.7999	H-5→ L+1 (11.173); H-4→ L (22.017); H-4→ L+1 (25.199); H-2→ L+4 (29.319); H→ L+1 (14.252); H→ L+5 (34.196)
	T_3	4.1889	H-9→ L+7 (12.986); **H-8→ L+1 (13.119); H-1→ L (50.013)**
	T_4	4.5768	H-2→ L+2 (44.264)
	T_5	4.5866	H-4→ L+4 (18.010); H-3→ L (11.140); H-2→ L (27.645); H-2→ L+1 (24.373); H→ L+2 (48.747)
Dimer-1	S_1	4.6431	**H-1→ L+2 (53.185)**
	T_1	3.6726	H-2→ L+1 (38.323)
	T_2	3.6744	H-6→ L+13 (17.717); H-4→ L+11 (17.789); H-3→ L+6 (29.741); H-3→ L+11 (13.647); H→ L+2 (32.928); H→ L+4 (35.454)
	T_3	3.7997	H-13→ L+1 (10.204); H-10→ L+1 (26.315); H-8→ L+3 (30.217); H-7→ L+7 (29.852); H-2→ L+1 (13.677)
	T_4	3.8008	H-9→ L+4 (10.749); H-6→ L+2 (17.683); H-6→ L+4 (24.447); H-4→ L+11 (13.071); H→ L+4 (12.290); H→ L+10 (11.144); H→ L+13 (30.034)
	T_5	4.1806	H-17→ L+15 (12.818); H-14→ L+4 (12.063); **H-1→ L+2 (49.960)**
	T_6	4.1911	H-16→ L (16.547); H-16→ L+1 (10.362); H-6→ L (19.159); H-6→ L+1 (10.723); H-5→ L (45.865); H-5→ L+1 (25.651); H-1→ L (11.777)
	T_7	4.5728	H-4→ L+6 (11.139); H→ L+2 (30.321); H→ L+4 (25.204)
	T_8	4.5752	H-8→ L+3 (11.874); H-8→ L+7 (25.705); H-7→ L+3 (43.019); H-2→ L+1 (27.076)
	T_9	4.5851	H-3→ L+2 (30.271); H-3→ L+4 (25.743); H→ L+6 (44.697)
	T_{10}	4.5860	H-8→ L (11.416); H-7→ L (23.399); H-2→ L+3 (47.806)
Dimer-2	S_1	4.6420	**H-3→ L+1 (22.162); H-3→ L+2 (37.881); H-2→ L (42.044)**

T_1	3.6584	H-9→ L+10 (10.205); H-8→ L+9 (10.235); H-7→ L+9 (10.469); H-6→ L+8 (11.639); H-6→ L+10 (10.672); H-5→ L+5 (21.310); H-1→ L+2 (16.316); H→ L (28.955); H→ L+4 (19.732)
T_2	3.6588	H-5→ L+3 (21.899); H-1→ L (28.599); H-1→ L+4 (19.893); H→ L+2 (15.735)
T_3	3.7922	H-9→ L (14.545); H-9→ L+4 (17.215); H-8→ L+1 (14.805); H-7→ L+2 (10.848); H-6→ L+3 (22.524); H-6→ L+9 (10.394); H→ L+10 (22.433)
T_4	3.7934	H-9→ L+2 (10.734); H-7→ L (11.382); H-7→ L+4 (14.779); H-6→ L+5 (20.955); H-5→ L+8 (18.781); H-4→ L+9 (21.923); H-1→ L+10 (21.722)
T_5	4.1827	**H-3→ L+1 (20.889); H-3→ L+2 (37.778); H-2→ L (37.656)**
T_6	4.1832	H-3→ L (37.411); H-2→ L+1 (21.110); H-2→ L+2 (37.798)
T_7	4.5532	H-5→ L (19.595); H-5→ L+3 (15.778); H-4→ L+1 (18.214); H-1→ L+3 (32.182); H→ L+5 (30.854)
T_8	4.5536	H-8→ L+9 (13.555); H-6→ L+8 (11.128); H-6→ L+10 (12.295); H-5→ L+5 (21.476); H-1→ L+1 (14.062); H-1→ L+5 (23.128); H→ L+3 (28.661)
T_9	4.5556	H-9→ L+5 (11.323); H-9→ L+8 (10.181); H-7→ L+3 (12.256); H-5→ L+2 (13.206); H-4→ L+3 (22.409); H-1→ L+5 (23.308); H→ L (22.752); H→ L+3 (22.963)
T_{10}	4.5560	H-9→ L+3 (11.019); H-8→ L+5 (10.842); H-8→ L+8 (10.047); H-7→ L+5 (11.337); H-7→ L+8 (14.506); H-6→ L+9 (14.689); H-4→ L+5 (25.184); H-1→ L (24.626); H-1→ L+3 (16.806); H→ L+5 (11.690)

[a]All triplet states (T_n) with orbital transition characteristics matching those of S_1 are highlighted in bold.

Table S8. Theoretical calculation results of AN–DBMI.

Aggregation state	Excited state	Excitation energy (eV)	Transition configuration (%)
Monomer	S_1	4.5610	**H-2→ L+1 (12.598); H→ L (68.690)**
	T_1	3.7472	H-4→ L+3 (11.584); H-4→ L+4 (16.311); H-3→ L+2 (11.826); H-2→ L (17.320); H-1→ L+3 (22.426); H→ L+2 (40.828)
	T_2	3.8257	H-3→ L+1 (11.318); H-2→ L+3 (12.549); H-1→ L+3 (24.874); H→ L+1 (12.880); H→ L+2 (19.528); H→ L+5 (32.355)
	T_3	4.2299	H-6→ L (13.326); H-5→ L+1 (32.506); H-4→ L+1 (20.233); **H-2→ L+1 (46.424)**
	T_4	4.3229	H-4→ L (35.506); H-2→ L (51.424); H-1→ L (15.427); H→ L+1 (11.319)
	T_5	4.3843	H-3→ L (22.038); **H→ L (59.597)**
	T_6	4.4538	H-6→ L+1 (25.299); H-5→ L (42.043); H-3→ L+1 (11.565); H-2→ L (20.558); H→ L+1 (15.007)
	T_7	4.5364	H-4→ L+3 (13.035); H-4→ L+4 (12.736); H-3→ L+1 (13.656); H-1→ L+3 (15.898); H→ L+1 (31.478)
Dimer-1	S_1	4.5485	**H→ L (51.408)**
	T_1	3.7438	H-7→ L+10 (11.471); H-6→ L+10 (11.444); H-3→ L+6 (13.879); H-1→ L+4 (20.052); H-1→ L+5 (19.752)
	T_2	3.7439	H-6→ L+10 (11.297); H-6→ L+11 (11.587); H-2→ L+6 (13.330); H-2→ L+7 (13.716); H-1→ L+5 (21.321); H→ L+5 (20.254)
	T_3	3.8232	H-7→ L+4 (15.293); H-7→ L+5 (14.658); H-6→ L+4 (14.955); H-6→ L+5 (14.788); H-3→ L+6 (14.496); H-3→ L+8 (15.501); H-3→ L+9 (15.395); H-1→ L+10 (15.933); H→ L+11 (16.626)
	T_4	3.8234	H-7→ L+4 (14.471); H-6→ L+5 (15.171); H-3→ L+8 (10.676); H-2→ L+8 (15.396); H-1→ L+10 (16.452); H-1→ L+11 (16.862); H→ L+10 (15.711); H→ L+11 (15.638)
	T_5	4.2828	H-15→ L+2 (12.415); H-13→ L+2 (10.204); H-12→ L (10.555); H-4→ L+2 (31.504)
	T_6	4.2851	H-15→ L+3 (10.817); H-13→ L+3 (11.418); H-4→ L+3 (30.956)
	T_7	4.3480	H-9→ L (28.518); H-5→ L (32.140); H-4→ L+1 (31.086)

	T_8	4.3485	H-9→ L+1 (28.702); H-5→ L+1 (31.290); H-4→ L (31.538)
	T_9	4.3707	H-7→ L+1 (14.000); H-6→ L (14.279); **H→ L (42.924)**
	T_{10}	4.3711	H-1→ L (42.409)
Dimer-2	S_1	4.4579	**H→ L+1 (65.936); H→ L+2 (18.129)**
	T_1	3.7317	H-3→ L+1 (11.491); H-3→ L+3 (10.696); H-3→ L+7 (13.654); H-3→ L+11 (11.211); H-2→ L+7 (17.800); H→ L+3 (17.730); H→ L+5 (38.936)
	T_2	3.7488	H-9→ L+8 (15.060); H-7→ L+2 (12.354); H-6→ L (16.166); H-6→ L+6 (15.760); H-4→ L+6 (16.539); H-3→ L+6 (13.818); H-1→ L+4 (40.263)
	T_3	3.8135	H-3→ L+5 (11.995); H-2→ L+10 (16.392); H→ L+3 (11.696); H→ L+11 (31.252)
	T_4	3.8265	H-9→ L+6 (17.416); H-8→ L+4 (15.893); H-7→ L+4 (24.043); H-5→ L+6 (15.780); H-5→ L+8 (10.812); H-4→ L+6 (15.655); H-4→ L+8 (18.201); H-3→ L+6 (11.814); H-3→ L+8 (14.764); H-1→ L+2 (12.339); H-1→ L+4 (17.985)
	T_5	4.2246	H-11→ L+1 (10.210); H-9→ L+2 (18.419); H-6→ L+2 (30.224)
	T_6	4.2289	H-8→ L+3 (18.700); H-5→ L+3 (10.004); H-3→ L+3 (30.837)
	T_7	4.3067	H-9→ L (31.444); H-6→ L (33.619)
	T_8	4.3215	H-7→ L+1 (19.933); H-4→ L+1 (32.407); H-4→ L+1 (11.335); H-2→ L+1 (12.001); H→ L+3 (11.030)
	T_9	4.3601	**H→ L+1 (55.743); H→ L+2 (15.738);** H→ L+7 (12.135)
	T_{10}	4.4007	H-6→ L (10.280); H-1→ L (55.504); H-1→ L+6 (12.373)

[a]All triplet states (T_n) with orbital transition characteristics matching those of S_1 are highlighted in bold.

References

[1] M. D. Li, N. K. Wong, J. Xiao, R. Zhu, L. Wu, S. Y. Dai, F. Chen, G. Huang, L. Xu, X. Bai, M. R. Geraskina, A. H. Winter, X. Chen, Y. Liu, W. Fang, D. Yang and D. L. Phillips, *J. Am. Chem. Soc.*, 2018, **140**, 15957.

[2] T. Lu and F. Chen, *J. Comput. Chem.*, 2012, **33**, 580.

[3] T. Lu and Q. Chen, *J. Comput. Chem.*, 2022, **43**, 539.

[4] C. Lefebvre, G. Rubez, H. Khartabil, J. C. Boisson, J. Contreras-Garcia and E. Henon, *Phys. Chem. Chem. Phys.*, 2017, **19**, 17928.